XIII International Conference on Computational Plasticity. Fundamentals and Applications
COMPLAS XIII
E. Oñate, D.R.J. Owen, D. Peric and M. Chiumenti (Eds)

# INFLUENCES OF YIELD CRITERIA ON STRESS BASED FORMING LIMIT DIAGRAM OF DP980 STEEL

**SANSOT PANICH[*] AND VITOON UTHAISANGSUK[†]**

[*] Department of Production Engineering, Faculty of Engineering,
King Mongkut's University of Technology North Bangkok
1518 Pracharat 1 Road, Wongsawang, Bangsue, Bangkok 10800, Thailand
Email: sansotp@kmutnb.ac.th, Web page: www.kmutnb.ac.th

[†] Department of Mechanical Engineering, Faculty of Engineering,
King Mongkut's University of Technology Thonburi
126 Pracha Uthit Road, Bang Mod, Thung Khru, Bangkok 10140, Thailand
Email: vitoon.uth@kmutt.ac.th, Web page: www.kmutt.ac.th

Keywords: Forming limit stress diagram, Marciniak–Kuczinsky model, Yield criteria, High strength steel.

**Abstract.** In this study, experimental and numerical determination of forming limit stress diagram (FLSD) for an advanced high strength (AHS) steel grade 980 were carried out. Forming limit curve (FLC) of the steel was first experimentally obtained by means of the Nakazima stretch –forming test. Then, analytical calculations of the FLSD were performed based on the Marciniak–Kuczynski (M–K) model. The FLSD was also directly computed by using the experimental FLC data. Different yield criteria, namely, Hill'48 (r–value and stress–based), Yld89 (r–value and stress–based) and Barlat2000 (Yld2000–2d) were examined, in which predicted plastic flow behaviors of the AHS steel in different directions were evaluated. Hereby, the strain hardening was described by the Swift law. Uniaxial tension, balanced bi–axial bulge test and in–plane biaxial tension test were performed for identifying material parameters of each yield model. Influences of the constitutive models, imperfection values and work hardening coefficient on the M−K based FLSDs were investigated in comparison that resulted from the FLC data. It was found that the predictions of stress based forming limits, especially in the biaxial state of stress, using the M–K theory were strongly affected by the yield function. The FLSD calculated by the Yld2000–2d criterion more acceptably agreed with the FLSD based on the experimental data than other model.

## 1 INTRODUCTION

The automotive industry has been continuously forced to design and produce vehicles under consideration of weight reduction, increased crash performance, energy saving and environmental aspect. Thickness reduction of steel sheets used in car bodies is desirable as it leads to vehicles with low fuel consumption and low $CO_2$ emission. On the other hand, passenger safety can be also enhanced by using steels with high energy absorption ability. Thus, the steel grades with higher strength and ductility are increasingly needed [1]. The

advanced high strength (AHS) steels apparently show major advantage according to their high strength to density ratio, however their formability is relatively low. More precise prediction of the forming limit of these steel grades is hence important. In this work, FLCs of the AHS dual phase (DP) steel grade DP980 were firstly experimentally determined by the Nakazima stretch−forming test. Then, corresponding FLSD was numerically calculated on the basis of these experimental data. Additionally, FLSDs of the steel were predicted by the M−K model [2]. The influences of different anisotropic yield functions, Hill's 48 stress based (Hill'48−S), Hill's 48 strain based (Hill'48−R) [3], Yld89 stress based (Yld89−S), Yld89 strain based (Yld89−R) [4] and Yld2000−2d [5] model on the forming limit stresses were studied. Effects of the imperfection, exponent of yield functions and work hardening coefficients values on the resulted forming limit stresses were also examined. Uniaxial tension, hydraulic bulge and in–plane biaxial tests were conducted for identifying necessary material parameters of each model. Finally, the FLSDs calculated from the experimental FLC data and predicted by the M−K model in combination with different anisotropic yield functions and model parameters were compared and discussed.

## 2 EXPERIMENTAL AND THEORETICAL STRESS BASED FORMING LIMIT

### 2.1 Stress based forming limit

It has been well reported that the FLC is sensitive to pre−forming conditions of steel sheets. By most industrial applications, complex parts are usually produced in multi−step forming processes. Thus, influences of non−proportional strain histories on the FLC can be critical. Under such conditions, obtained FLC cannot be applied to predict whether the forming process will be successful. In contrast, the stress based forming limit is represented by the principal in−plane stress components developed on a sheet metal. It was found that the FLSD is more robust against any changes of strain paths occurring in a forming process [6].

A brief description for determining the limit stress values are shown as following. First, the strain path is thus characterized by the strain ratio [7].

$$\rho = \varepsilon_2/\varepsilon_1 \tag{1}$$

The stress ratio is defined as:

$$\alpha = \sigma_2/\sigma_1 \tag{2}$$

For materials is in-plane isotropic,the shear stress is absent in a coordinate system aligning with the anisotropy axes,the major and minor true stresses can be expressed as following.
The major true stress is described as:

$$\sigma_1 = \overline{\sigma}(\overline{\varepsilon})/\xi(\alpha) \tag{3}$$

and the minor true stress is expressed as:

$$\sigma_2 = \alpha\sigma_1 \tag{4}$$

Which $\bar{\sigma}(\bar{\varepsilon})$ is an effective stress computed with regard to a hardening law, $\xi(\alpha)$ represents a function of material parameters and $\alpha$ is calculated from each applied anisotropic yield criterion. As seen, the FLSDs obatined from the experimental FLC data likely depends on the shape of the yield surface and hardening law used to describe local plastic deformation of the investigated steel [7].

## 2.2 Experimental stress based forming limit

To determine the experimental stress based forming limit diagram (FLSDs based on experimental FLC data), FLC of the steel DP980 was firstly obtained by performing the Nakazima stretch−forming test according to the international standard ISO 120004−2 [8] on a 600 kN Erichsen sheet metal testing machine. The schematic of the Nakazima test setup is illustrated in Fig. 1a. The tested sheet samples had the initial thickness of 1.2 mm and the same length of 190 mm, but different widths varying from 55 to 195 mm, as demonstrated in Fig. 1a. The deformed samples after forming until fracture were depicted in Fig. 1b. The experimental procedure of the Nakazima test was described in details in [7,9]. During the tests, local strain distributions on the samples were measured by means of the AutoGrid optical system. Since stress values could not be directly determined from the experiments, forming limit stresses were then computed for various states of stress on the basis of the experimental limit strains, plasticity theory with different yield criteria and hardening laws. The proposed method for transformation between strain and stress space was given in details in section 2.1 and [7,10].

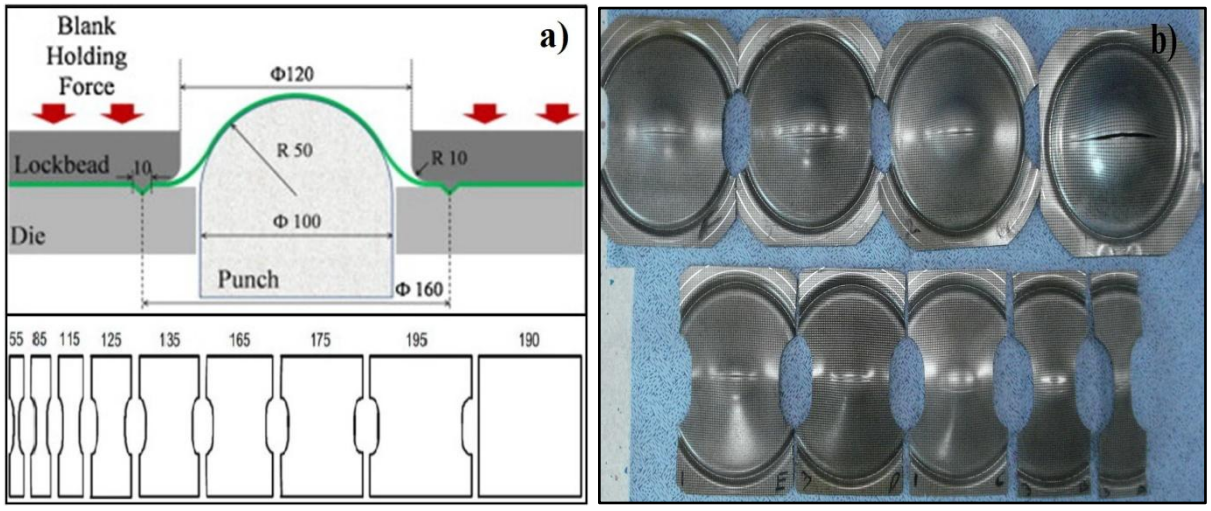


**Figure 1**: a) Schematic of the Nakazima test setup and used sample dimension and b) formed Nakazima samples after failure

## 2.3 Theoretical stress based forming limit

Calculation of local plastic instability of the formed steel sheet was done by using the M−K theory [2]. The model has been widely applied for predicting forming limit of sheet metals. By the M−K theory, steel sheet is considered as a heterogeneous material, in which

occurred localized necking was evaluated through a critical value with respect to thickness ratio in a local area. Initially, the theoretical model was used to predict the right hand side of the FLC. Then, Marciniak and Kuczynski modified the model by assuming an initial imperfection oriented at 90° to the principal major stress direction in the sheet, as shown in Fig. 2, and localized necking develops from this.

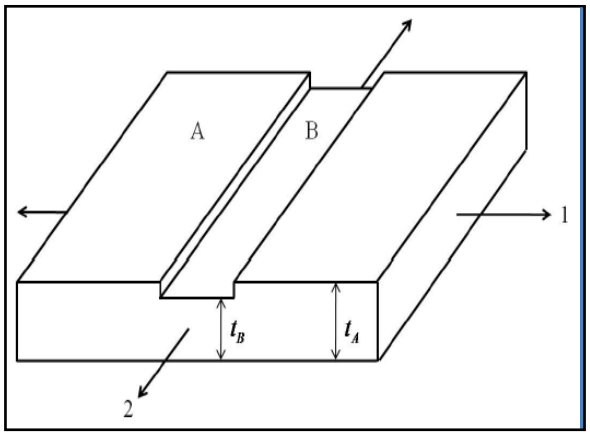


**Figure 2**: A schematic of the M−K model characterized by an initial groove

The initial imperfection is characterized by the thickness ratio ($f = t_B / t_A$). Compatibility condition requires that the strains parallel to the groove are equal in both regions.

$$\varepsilon_{2\mathrm{A}} = \varepsilon_{2\mathrm{B}} \tag{5}$$

The force balance across the groove should be satisfied as following.

$$\sigma_{1\mathrm{A}} t_{\mathrm{A}} = \sigma_{2\mathrm{B}} t_{\mathrm{B}} \tag{6}$$

In the imperfection model purposed by Marciniak–Kuczynski, it is assumed that the stress ratio ($\alpha = \sigma_2 / \sigma_1$) is constant during the whole deformation process. When the ratio of the strain increments along the direction 1 in the imperfection region ($\Delta\varepsilon_{1\mathrm{B}}$) to the strain increments along the direction 1 in the homogeneous region ($\Delta\varepsilon_{2\mathrm{B}}$) drops below 0.1, it is presumed that localized necking just occurs. When the necking criterion was reached, the calculation was terminated and corresponding strains and stresses accumulated in the homogeneous zone at that moment were taken into account as the limit strains and limit stresses. Theoretical concept of M–K based analysis was presented in details in [2,7,10]. The FLSDs of the investigated steel were predicted by using the M−K model in combination with the Hill'48 (*r*−value and stress−based), Yld89 (*r*−value and stress−based) and Yld2000−2d yield criteria.

## 3 MATERIALS MODEL

### 3.1 Hill'48 yield criterion

A quadratic anisotropic yield criterion was proposed by Hill [3] in 1948 that became one of the most widely used yield functions. Materials parameters of the Hill's 48 model represented a plane stress state, which was a good approximation for sheet metal forming process, as expressed in Eq. 7.

$$2f(\sigma) = (G+H)\sigma_{xx}{}^2 + (F+H)\sigma_{yy}{}^2 - 2H\sigma_{xx}\sigma_{yy} + 2N\sigma_{xy}^2 = 1 \tag{7}$$

$F$, $G$, $H$ and $N$ are the anisotropic coefficients. It could be directly obtained from the calculation of the determined yield stresses or $r$–values of the concerned material. For the Hill's 48 criterion based on stress (Hill'48–S), required parameters were the uniaxial yield stresses at 0°,45° and 90° to the rolling direction (RD) and the balanced biaxial yield stress. By the Hill's 48 model based on $r$–value (Hill'48–R), materials parameters were indeed the uniaxial yield stress at the RD and the $r$–values at 0°, 45° and 90° to the RD.

### 3.2 Yld89 yield criterion

The non quadratic anisotropic yield criterion proposed by Barlat and Lian [4] in 1989 is a plane stress anisotropic yield function, as described in Eq. 8.

$$f(\sigma) = a|K_1 + K_2|^M + a|K_1 - K_2|^M + c|2K_2|^M = 2\bar{\sigma}^M \tag{8}$$

Where $K_1 = \frac{\sigma_{xx} + h\sigma_{yy}}{2}, K_2 = \sqrt{\left(\frac{\sigma_{xx} - h\sigma_{yy}}{2}\right) + (p\sigma_{xy})^2}$ , $M$, $a$, $c$, $p$ and $h$ are the representative anisotropic yeild parameters. By the same manner, for the Yld89 stress based (Yld89–S) model, these anisotropic coefficients could be identified from the uniaxial yield stresses at 0° and 90° to the RD and the balanced biaxial yield stress. Otherwise, for the Yld89 strain based (Yld89–R) criterion the uniaxial yield stresses at the RD and $r$–values at 0° and 90° to the RD as described in [4,11] were required.

### 3.3 Yld2000–2d yield criterion

The well known non–quadratic anisotropic yield function introduced by Barlat et al. [5] was employed to describe anisotropic behaviour of the examined DP980 steel sheet. The Yld2000-2d yield criterion could be described under a plane stress assumption in Eq. 9.

$$f(\sigma) = \left|S_1' - S_2'\right|^M + \left|2S_2'' + S_1''\right|^M + \left|2S_1'' + S_2''\right|^M = 2\bar{\sigma}^M \tag{9}$$

Where $S_i'$ and $S_i''$ are the principal values of the stress tensors $S'$ and $S''$. In case of the Yld2000–2d anisotropic yield criterion, the requested materials parameters were the uniaxial yield stresses and the $r$–values at 0°, 45°, and 90° to the RD, the balanced biaxial yield stress and the balanced biaxial $r_b$ value. These eight properties, precisely, yield stresses $\sigma_0$, $\sigma_{45}$, $\sigma_{90}$ and $\sigma_b$, and $r$–values $r_0$, $r_{45}$, $r_{90}$ and $r_b$ were experimentally determined and used to calculate anisotropic coefficients of the yield function.

### 3.4 Hardening law

The Swift hardening law, as expressed in Eq. 10 was applied to describe the stress–strain curve obtained from the tensile test in the RD for the examined DP980 steel.

$$\bar{\sigma} = K\left(\bar{\varepsilon}_o + \bar{\varepsilon}_p\right)^n \tag{10}$$

Where $\bar{\sigma}$ and $\bar{\varepsilon}_p$ are the effective stress and plastic strain, respectively. $K$, $n$ and $\varepsilon_o$ are the material constants, which were determined by the regression method with the experimentally determined stress–strain curves from the uniaxial tensile test.

## 4. MATERIALS CHARACTERIZATION

### 4.1 Uniaxial tensile test

Uniaxial tensile tests of the investigated DP980 steel were performed on a MTS universal testing machine using the ASTM E8 standard specimen. The samples were tested under three loading directions, 0°, 45° and 90° to the RD. During the tension tests, elongations within gauge length of the sample in both sample length and width were measured. The constant strain rate of 0.001 $s^{-1}$ was applied and kept during the whole test. The *r*–values were calculated at the total elongation of 14%. The normalized yield stresses and *r*–values of the examined steel for different directions were presented in Table 1.

**Table 1** Normalized yield stresses and *r*–values of the examined DP980 steel

| DP980 | 0° | 45° | 90° | Balanced biaxial |
|---|---|---|---|---|
| Normalized flow stress | 1.0000 | 0.9822 | 0.9943 | 1.0876 |
| *r*–value | 0.8407 | 1.0516 | 0.9497 | 1.3335 |

### 4.2 Hydraulic bulge test

Hydraulic bulge tests were carried out on an Erichsen testing machine, in which biaxial flow behaviours of the material could be characterized. The experimental procedure and geometry of tooling could be found in [12]. During the tests, membrane stresses and thickness strains were simultaneously calculated. The hydraulic pressure was continuously increased until it suddenly dropped because of crack appearance. The balanced biaxial yield stress ($\sigma_b$) for the DP980 steel was illustrated in comparison with the tensile curves in [13]. The balanced biaxial yield stresses were normalized by the uniaxial yield stress from the RD and given in Table 1.

### 4.3 In-plane biaxial tension test

An in–plane biaxial tension tester developed by Kuwabara [14] was conducted for determining plastic deformation behaviour under the biaxial state and for computing the balanced *r*–value ($r_b$). As illustrated in Fig. 3a, the tester has two pairs of cylinders aligned in both the x– and y–axes. Each arm is equipped with a load cell to measure the tensile force in each loading direction. In Fig. 3b, dimension of the test specimen, which has seven slits on

each arm along both loading directions, is shown. The slits release the geometric constraints due to the deformation in the transverse direction of the each gauge section. The plastic strains were measured using strain gauges that were attached on the surface of the gauge section of the cruciform specimens. The strain rate was about 0.001 $s^{-1}$. The balanced biaxial load test was repeated three times to obtain reliable results. The experimental procedure was expressed in details in [9,14]. The averaged $r_b$ was also shown in Table 1.

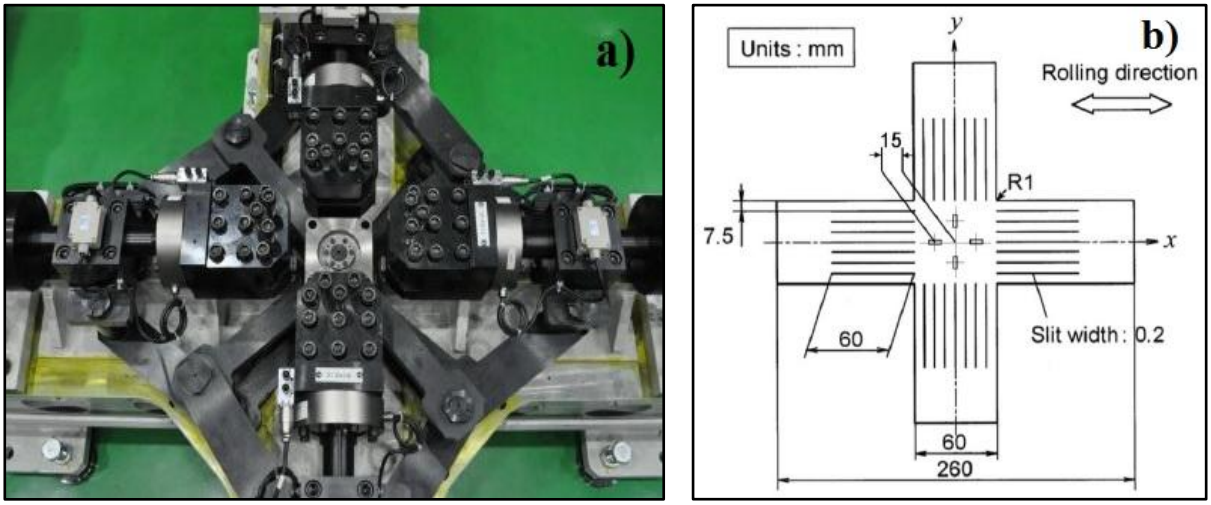


**Figure 3**: a) In–plane biaxial testing machine and b) Cruciform specimens and attachment of strain gauges for the in–plane biaxial tension test [9]

## 5. RESULTS AND DISCUSSION

### 5.1 Anisotropic characterization

The anisotropy of the investigated steel was characterized by menas of the determined yield stresses and *r*–values, for which different yield functions were considered. All required mechanical testing was described in section 3.1–3.3. Then, anisotropy coefficients of the yield functions, Hill's 48–R, Hill's 48–S, Yld89–R, Yld89–S and Yld2000–2d, were calculated by using the experimental data from Table 1. All obatined coefficients were demonstrated in Table 2–4. Since the DP980 steel mainly showed a microstructure consisting of ferrite, martensite and small amount of bainite, the exponent of the Yld2000–2d model was set to be 6 and 7, as recommended for BCC crystal structures [15,16]. The strain hardening behavior of the DP980 steel was decribed using the Swift hardening law [7,9]. Here, biaxial stress–strain curve obtained from the hydraulic bulge test was used in the model that was usually more suitable for representing state of stress in most sheet forming processes. Subsequently, predicted results were compared with the experimental ones in term of the normalized yield stress and *r*–values depending on the testing direction, as reported in [13].

**Table 2** Calculated anisotropic coefficients of the Hill'48 criterion for the DP980 steel

| Hill'48 | *F* | *G* | *H* | *N* |
|---|---|---|---|---|
| stress based | 0.42844 | 0.41695 | 0.58305 | 1.65045 |
| *r*–value based | 0.48092 | 0.54327 | 0.45673 | 1.58913 |

**Table 3** Calculated anisotropic coefficients of the Yld89 model for the DP980 steel

| Yld89 | *a* | *c* | *h* | *p* |
|---|---|---|---|---|
| stress based | 0.59384 | 1.40615 | 1.00578 | 1.02073 |
| *r*–value based | 1.05666 | 0.94334 | 0.96832 | 1.02592 |

**Table 4** Calculated anisotropic coefficients of the Yld2000–2d model with M = 6 and 7 for the DP980 steel.

| Yld2000–2d | $\alpha_1$ | $\alpha_2$ | $\alpha_3$ | $\alpha_4$ | $\alpha_5$ | $\alpha_6$ | $\alpha_7$ | $\alpha_8$ |
|---|---|---|---|---|---|---|---|---|
| M=6 | 0.85244 | 1.08058 | 0.89426 | 0.97875 | 0.96722 | 0.71138 | 1.00047 | 1.15072 |
| M=7 | 0.90052 | 1.04654 | 0.87116 | 0.97773 | 0.96579 | 0.74660 | 1.00358 | 1.14479 |

## 5.2 Predicted forming limit stress diagram

The FLC of the examined DP980 steel was determined by the Nakazima test with the AutoGrid strain measurement system and then demonstrated in Fig. 4a. After that, calculations based on plasticity theory were performed for obtaing forming limit stresses of the examined steel. The influences of combinations of different yield criterion and the Swift hardening law on predicted threshold stresses were studied. First, FLSDs of the DP980 steel was computed with regard to the experimental forming limit curve of the steel. Fig. 4b illustrates the effects of the yield functions on the FLSDs determined from the FLC data. Obviously, the FLSDs obtained by using the Hill'48–S and Yld89–S yield criterion overestimated the FLSD calculated by the Yld2000–2d model. However, these FLSDs agreed well with that by the Yld2000–2d function in the biaixial state (at the right end of the curve), since the balanced biaxial yield stress value was taken into account in these both applied yield models. On the other hand, the calculated FLSDs based on the Hill'48–R and Yld89–R much differed from the results obtained from the Yld2000–2d model in the biaxial region. This was likely due to that only the uniaxial yield stress was used in the calculations. Different types of yield criterion provided slightly deviated forming limit stress curves. In contrast, the yield model based on stress and *r*–value significantly exhibited different threshold stress curves.

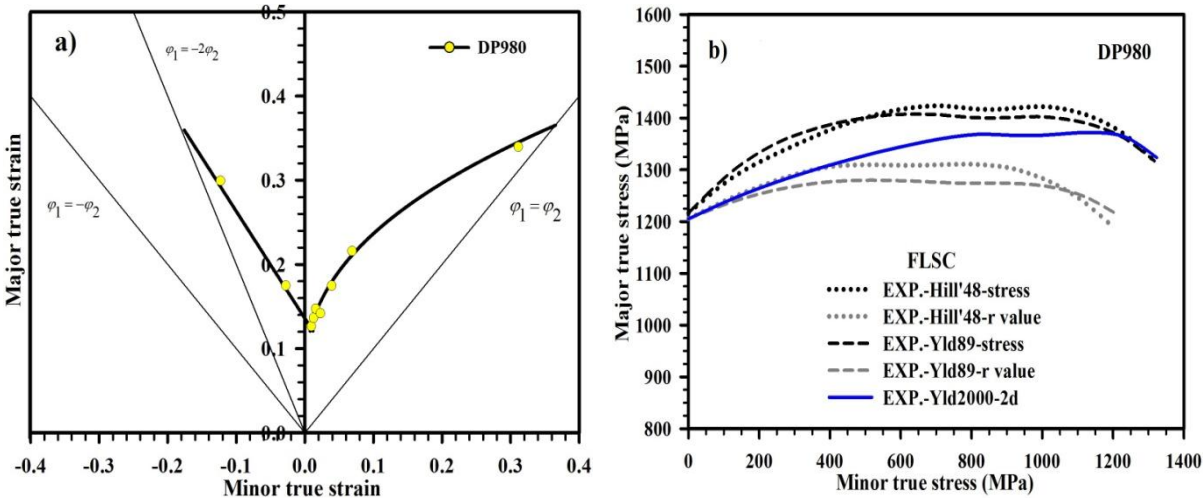


**Figure 4**: a) Experimentally determined FLC and b) Comparison between calculated FLSDs based on the experimental FLC data and different yield criteria of the DP980 steel.

Fig. 5a demonstrated the FLSDs, which were calculated on the basis of the experimental FLC data and the M–K model by applying the Swift hardening law coupled with different yield criteria, were compared. The M–K model was employed to identify the critical stresses for various states of stress. In this case, the initial imperfection parameter $f_0$ of 0.9995 [7,13] was defined and the exponent of the Yld2000–2d, Yld89–S and Yld89–R were set to be 6. It was found that the forming limit stress curve obtained by the combination of the M–K model and the Swift law coupled with the Yld2000–2d criterion better agreed with the FLSD based on the FLC than other yield models. However, from the plane strain to biaxial state, the calculated curve showed apparent overestimation. The other yield functions also exhibited deviations in these stress ranges, but with much higher magnitudes. From the uniaxial to plane strain state, or particularly in the uniaxial tension range, all predicted curves just slightly underestimated the experimental limit stresses. Additionally, in the stress range between uniaxial to plane strain state, the predicted limit stress curves from the Hill'48–R and Yld89–R a bit differed from the FLSDs based on the FLC data, but the resulted curves from the Hill'48–S and the Yld89–S showed larger deviations, since the yield stresses and *r*–values in some directions were not taken into account here.

Fig. 5b depicted the FLSDs based on the experimental FLC in comparison with the FLSDs based on the M–K theory coupled with the Yld2000–2d and Yld89 models using the *M* exponent of 6 and 7. Obvious deviations between the limit stresses, which were obtained by using both *M* exponent values were found for all yield functions. It can be seen that from the uniaxial to plane strain state, all yield models applying the *M* exponent of 6 could more fairly described the experimentally based FLSD than those applying the *M* exponent of 7. In contrast, from the plane strain to biaxial state, the limit stress curves resulted by the *M* exponent of 7 were closer to the experimental limit stress curve than those obtained by the *M* exponent of 6 for the Yld89–R and Yld 89–S and Yld2000–2d models.

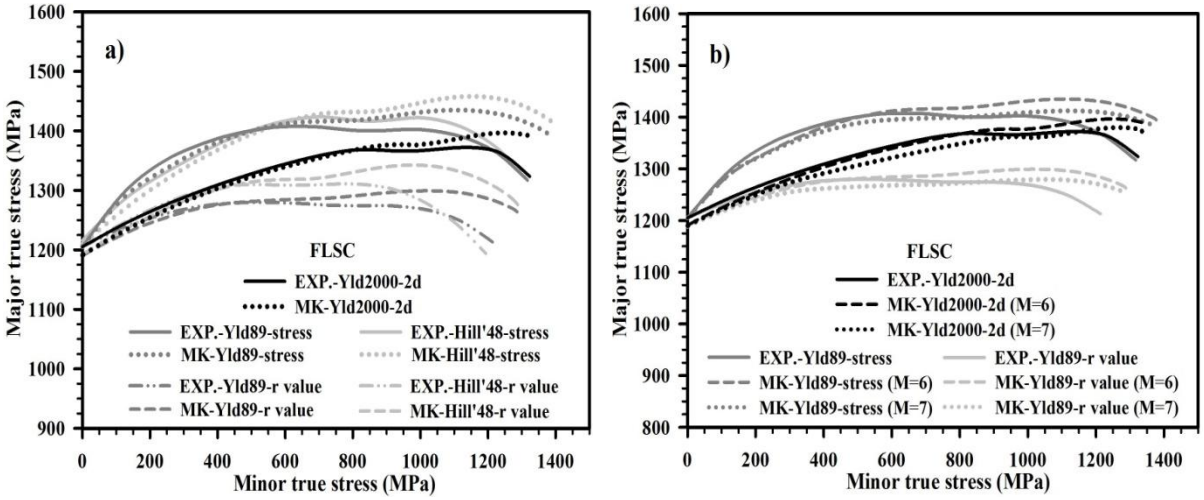


**Figure 5**: Comparison between determined FLSDs based on the experimental FLC and the M-K model: a) with all yield criteria in comparison and b) with the Yld89 and Yld2000–2d model and the M exponent of 6 and 7

It is known that the geometric defect in the M–K analysis is conventional and not a real physical attribute of the specimen. Many researchers reported that, the imperfection value $f_0$ could affect the yield surface shape and resulting limit strain and stress curve. Note that, in this work, an unique imperfection factor was used for fitting the best condition to study the other effects as mentioned. However, the influences of the imperfection on the calculated FLSDs are illustrated in Fig. 6a. It was found that increasing the imperfection value led to an increase of the calculated forming limit stresses in all states of stress from the uniaxial tension to biaxial strain state. For for the M–K model based calculations in this work, the imperfection value of 0.9995 was identified with regard to the Yld2000–2d criterion, in which the limit curve predicted by this value was mostly close to the limit stress curve based on the FLC data. The imperfection value higher than 0.9995 provided the calculated limit stress curves higher than the one based on the FLC in the plane strain to biaxial state, but the imperfection value lower than 0.9995 showed the reciprocal effect.

Furthermore, influences of the work hardening coefficient (*n*–value), which strongly depended on whether used stress–strain curves were obtained from the biaxial or uniaxial tensile tests. In this work, the *n*–value of 0.044 and 0.059 were determined from the biaxial and uniaxial tensile test data for the DP980 steel, respectively. Here, FLSDs, which were calculated by using the Yld2000–2d, Hill'48–S and Hill'48–R models under consideration of both *n*–values, were compared in Fig. 6b. Obviously, the work hardening coefficient obtained from the biaxial stress–strain response provided the forming limit stress curves closer to the limit stress curve based on the FLC data than those using the uniaxial tension stress–strain curve for all concerned yield functions in the uniaxial to plane strain state. Otherwise, there were larger deviations from the plane strain to biaxial state for every yield criteria, since yield stresses or *r*–value in every direction were completely used. The calculated FLSDs from the Hill'48–S model were definitely higher than those based on the Hill'48–R model. The calculated limit stresses decreased at all states of deformation, when the higher *n*–value was applied for all investigated yield criteria.

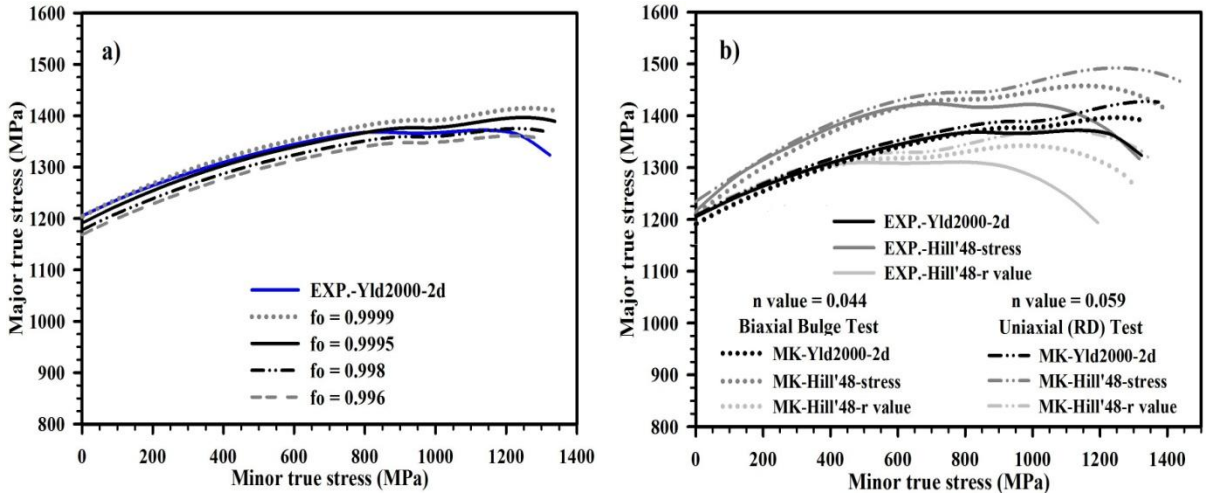


**Figure 6**: Comparison between determined FLSDs based on the experimental FLC and the M–K model coupled with a) the Yld2000–2d model applying different imperfection values and b) the Hill'48–S, Hill'48–R and Yld2000–2d models and different work hardening coefficients

## 6. CONCLUSIONS

The strain based forming limit diagram of the AHS steel grade DP980 was experimentally determined by the Nakazima stretch–forming test. Then, the FLSDs were calculated on the basis of the experimental FLC data in combination with various yield criteria. The FLSDs were also determined by applying the M–K model coupled with the Swift hardening law in combination with the Yld2000–2d, Yld89 stress based, Yld89 strain based, Hill'48 stress based and Hill'48 stress based yield criteria. The influences of anisotropic yield functions on the calculated limit stress curves were demonstrated. The *M* exponent in the Yld2000–2d and Yld89 models showed significant effects on the obtained FLSDs in the plane strain to biaxial state. The imperfection value also strongly affected the calculated limit stresses in the whole stress ranges. Different work hardening coefficients led to deviated FLSD predictions, especially from the plane strain to biaxial state. For the examined DP980 steel, the Yld2000–2d model using the *M* exponent of 6 and the imperfection value of 0.9995 coupled with the Swift hardening law could more precisely described the FLSDs based on the FLC data than other model combinations. For a more accurate FLSD prediction based on the M–K theory, especially for the plane strain to biaxial state, the applied yield criterion, in which yield stresses and *r*–values in different directions were required, must be precisely investigated.

## ACKNOWLEDGEMENTS

The authors would like to acknowledge the Faculty of Engineering, King Mongkut's University of Technology North Bangkok for the financial supports.The authors also wish to express their gratitude to Prof. Frédéric Barlat (Pohang University of Science and Technology) for all supporting and useful discussion. Moreover, the authors are grateful to POSCO for the supplied material DP980 steel sheets. Obviously, the author is so thankful to members of Materials Mechanics Laboratory, GIFT, POSTECH for their support and help.

## REFERENCES


[1] Uthaisangsuk, V., Muenstermann, S., Prahl, U., Bleck, W., Schmitz, H.P. and Pretorius, T. A study of microcrack formation in multiphase steel using representative volume element and damage mechanics. Comp. Mater. Sci. (2011) 50:1225-1232.

[2] Marciniak, Z and Kuczynski, K. Limit strains in the processes of stretch-forming sheet metal. Int. J. Mech. Sci. (1967) 9: 609-612.

[3] Hill, R. A theory of the yielding and plastic flow of anisotropic metals. In: Proceeding of Royal Society London A. (1948) 193:281-297.

[4] Barlat, F. and Lian, J. Plastic behavior and stretchability of sheet metals. Part I: A yield function for orthotropic sheets under plane stress conditions. Int. J. Plast. (1989) 5:51-66.

[5] Barlat, F., Brem, J.C., Yoon, J.W., Chung, K., Dick, R.E, Lege, D.J., Pourboghart, F., Choi, S.H. and Chu, E: Plane stress yield function for aluminum alloy sheets - Part 1: Theory. Int. J. Plast. (2003) 19:1297-1319.

[6] Uthaisangsuk, V., Prahl, U., Mueunstermann, S. and Bleck, W. Experimental and numerical failure criterion for formability prediction in sheet metal forming. Comput. Mater. Sci. (2008) 43:43-50.

[7] Panich, S., Barlat, F. Uthaisangsuk, V. Suranantchai, S. Jirathearanat, S. Experimental and theoretical formability analysis using strain and stress based forming limit diagram for advanced high strength steels. Mater. Des. (2013) 51:756-766.

[8] International Standard ISO 12004-2 Metallic materials - Sheet and strip – Determination of forming-limit curves. Part 2: Determination of forming-limit curves in the laboratory, (2008).

[9] Kim, S.N., Lee, J.W., Barlat, F. and Lee, M.G. Formability prediction of advanced high strength steels using constitutive models characterized by uniaxial and biaxial experiments. J. Mater. Proc. Tech. (2013) 213:1929-1942.

[10] Butuc, M. C., Gracio, J. J. And Da Rocha, A. B. An experimental and theoretical analysis on the application of stress-based forming limit criterion. Int. J. Mech. Sci. (2006) 48:414–429.

[11] Dasappa, P., Inal, K. and Mishra. R. The effects of anisotropic yield functions and their material parameters on prediction of forming limit diagrams. Int. J. Sol. Struc. 49 (2012) 49:3528-3550.

[12] Young, R.F., Bird, J.E. and Duncan, J.L. An automated hydraulic bulge tester. J. Applied Metalworking. (1981) 2:11-18.

[13] Panich, S. and Uthaisangsuk, V. Effects of anisotropic yield functions on prediction of forming limit diagram for AHS steel. Key. Eng. Mater. 2014 pp 257-264.

[14] Kuwabara, T., Ikeda, S., Kuroda, K. Measurement and analysis of differential work hardening in cold-rolled steel sheet under biaxial tension. J. Mater. Proc. Tech.(1998) 80–81:517–523.

[15] Hosford, W. F. On yield loci of anisotropic cubic metals. In Proceedings of 7th North American Metalworking Conf. SME, Dearborn, MI (1979) 191-197.

[16] Kuwabara, T., Hashimot, K., lizuka, E. and Yoon. J.W. Effect of anisotropic yield functions on the accuracy of hole expansion simulations. J. Mater. Proc. Tech. (2011) 211:475-481.
[17] Butuc, M. C., Gracio, J.J. and da Rocha, A.B. A theoretical study on forming limit diagrams prediction. J. Mater. Proc. Tech. (2003) 142:714-724.